

Cite this: *RSC Mechanochem.*, 2026, 3, 33Received 29th August 2025
Accepted 25th November 2025

DOI: 10.1039/d5mr00110b

rsc.li/RSCMechanochem

Shedding water: using mechanochemistry to drive liquid assisted synthesis of the energetic complex glycine–magnesium tetrahydrate

Tristan W. Kenny and Lori J. Groven *

In this effort, a solvent-free, media-free, mechanochemical route is used to accelerate the synthesis and exploration of an energetic oxidizer: fuel complex. Using magnesium nitrate hexahydrate and glycine as our example, we demonstrate that water from the metal salt is shed with moderate energy input and drives liquid-assisted mechanochemistry. This route reduces synthesis time from days to hours and shows promise for a host of metal salt complexes.

Metal salt complexes are widely used for various applications, from agricultural to battery technologies.^{1–3} A recent area of interest uses metal salt complexes to synthesize metal oxides through a combustion route.⁴ These can be used as a sorbent and/or as catalyst for the decomposition of organophosphates.^{5,6} The primary issue when considering the synthesis is that many metal salts, along with the polar organic molecules they are complexed with, are hygroscopic, which makes the traditional water-based synthesis take days to weeks.⁷ A mechanochemical synthesis method could eliminate the addition of water as part of the synthesis process, hence reducing the synthesis time.

Mechanochemical synthesis typically uses a fraction of the water for liquid-assisted grinding methods, and solvent-free methods eliminate the addition of water.^{8,9} Hydrated metal salts have weakly bonded waters and can shed them with relative ease, hence, the simple impact between reactants during crystal–crystal impact may be sufficient to initiate reaction.^{10–12} Previously reported metal salt complexes have shown that for successful complex formation, there is displacement of the crystalline water in the metal salt structure.^{7,13} Therefore, if mixing induces the shedding of water, then this water could drive liquid-assisted mechanochemistry, and allow quick product formation, while eliminating the excessive drying time necessary with evaporative routes.

This effort targets the formation of the known 1 : 1 mole ratio magnesium nitrate:glycine complex, catena-poly[[[tetra-aquamagnesium(II)]-μ-glycine-κ²O:O'] dinitrate], which will be referred to as mgn-gly complex.⁷ This allows direct comparison to the reported products from traditional solvent (aqueous) evaporation synthesis.^{4,7} The two reactants will be mixed in a LabRAM at selected times to observe the role of time on the resulting product formation, at a fixed acceleration. The products will be dried at 60 °C and then examined using powder X-ray Diffraction (*p*-XRD), Fourier Transform Infrared spectroscopy (FTIR), and Differential Scanning Calorimetry with Thermogravimetric Analysis (DSC-TGA). Additionally, the synthesized complexes will be reacted, and the products collected. The combustion product will then undergo BET specific surface area analysis to compare synthesis routes.

Materials were mixed in 2-gram batches (1.55 g magnesium nitrate hexahydrate from Sigma-Aldrich and 0.45 g α -phase glycine from Sigma-Aldrich) at 30 g's acceleration for 15 minutes, 30 minutes, and 1 hour. After mixing, the materials were examined for indicators of new material formation (phase change, color change, *etc.*). A comparison batch of solvent evaporation (SE) crystals were also synthesized, and the bulk products were analyzed. The SE crystals use the same mass of magnesium nitrate hexahydrate and glycine but are solubilized in 10 mL of water and then dried at 60 °C for three days.

During mixing, there were appearance indicators that a new material had formed after just 30 minutes. As shown in Fig. 1, the material started as a free-flowing powder, and then, after 30

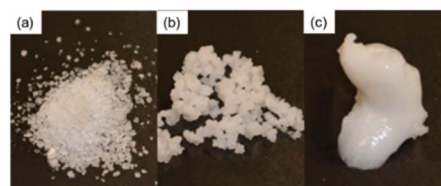


Fig. 1 Images of the mixture at (a) 0 minutes, (b) 30 minutes, and (c) 1 hour.

Karen M. Swindler Department of Chemical and Biological Engineering, South Dakota School of Mines and Technology, Rapid City, SD, USA. E-mail: lori.groven@sdsmt.edu



minutes, wet agglomerates were observed, indicating enhanced interaction as a result of the water shed from the magnesium nitrate hexahydrate. After 1 hour, the materials clumped together, forming a single wet mass. This is also observed as the LabRAM power output is plotted *versus* time (provided in the supplemental) which indicates agglomeration occurring around 45 minutes, further indicating new material formation and that indeed the water from the magnesium nitrate hexahydrate was shed during milling. This shifts the process from dry to a liquid-assisted synthesis route, significantly enhancing diffusion and reactant interaction as milling time increases.

To validate this, dehydrated magnesium nitrate hexahydrate, and glycine were also processed. In this case, after an hour of mixing the material remained a dry white powder. While this does not exclude the possibility of product formation due to solid state diffusion, there was no qualitative change to indicate any reaction occurred. A significant difference in moisture content was observed between a physical mixture of the as-received material and a dehydrated physical mixture. The dehydrated magnesium nitrate hexahydrate : glycine physical mixture lost 3.90% while the as-received material lost 12.03% of its mass. The mass loss of the as-received material is close to the expected mass loss for losing two of the waters (10.87%), suggesting the hydration state plays a role in the synthesis.

The pXRD (Fig. 2) compares the mechanochemical (MC) crystals diffraction pattern to the diffraction pattern of the previously confirmed mgn-gly complex synthesized using the solvent evaporation method. The powder diffraction patterns indicate that the MC product resulted in a crystal structure similar to the confirmed complex, as both exhibit unique peaks at 9° and 10°. There are several peaks, around 15°, in the SE crystal diffraction pattern which were not observed for the MC crystals. When the MC crystal diffraction pattern is compared to the constituents' diffraction patterns, magnesium nitrate hexahydrate and glycine, the absence of the constituent peaks strongly indicates that this method produced a more phase pure product over the SE method. The diffraction pattern of the physical mixture shows a minor peak at 10° indicative of some material reacting to form the desired product but is

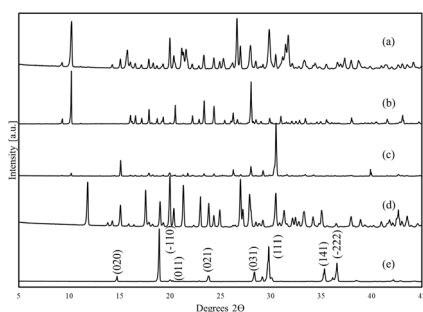


Fig. 2 Magnesium nitrate : glycine pXRD with the product peaks being confirmed from CSD REFCODE TAWMOU⁷ (a) SE products, (b) MC products, (c) dried lab RAM of constituents (d) magnesium nitrate hexahydrate with peaks confirmed from Mozzi (1961) ICSD 23220,¹⁴ (e) as-received glycine with peaks confirmed from Hanawalt *et al.* (1938).¹⁵

Table 1 Estimations of the weight percent of the targeted complex and reactants from the different synthesis methods and mixing times from the Rietveld refinements (using the Jade 7.0 software)

Material	Mgn-gly [wt%]	Mgn·6H ₂ O [wt%]	Glycine [wt%]
MC product	97.2 ± 3.7	2.8 ± 1.3	0
SE product	80.4 ± 2.3	16.5 ± 1.8	3.1 ± 0.8
30 min	95.7 ± 4.9	5.9 ± 1.5	0
15 min	94.5 ± 4.5	4.3 ± 0.8	0
Dehydrated 1 h	1.6 ± 0.1	2.6 ± 0.2	95.9 ± 2.0
LabRAM			
As received physical mix	0.0	99.2 ± 16.0	0.8 ± 2.0

predominantly unreacted constituent components, with its dominate peak at 31° (a major peak for magnesium nitrate hexahydrate). Powder X-ray diffraction of all synthesized crystals can be found in the supplemental.

Rietveld analysis allowed for estimations of the composition of the bulk product as shown in Table 1. Analysis of the SE products indicate ~80 wt% of the desired product was present. For the LabRAM products, the product purity starts at 95%, increasing to 97% from 15 minutes to 1 hour. The dehydrated material is only 1.6% the complex, indicating the reaction was not driven by humidity as previously observed with organic complexes.¹² Analysis of just the physical mixture, that was mixed briefly prior to being scanned, shows no mgn-gly present and the predominant material being magnesium nitrate, a result of the significant portion of the physical mixture being magnesium nitrate. These results indicate that the MC products are more phase pure than the SE products. However, there are unaccounted amorphous materials and potential variation in sampling that could artificially alter the apparent composition of the products.

The synthesized product was further characterized with FTIR, as shown in Fig. 3. The SE crystals had peaks unique to the product's structure while also sharing peaks of the constituent components, as expected from the mgn-gly complex maintaining bonding of the constituents. This is further emphasized by the peaks associated with the hydration of magnesium nitrate hexahydrate, 3000–3600 cm⁻¹. The peaks associated with the hydration shift and decrease due to the

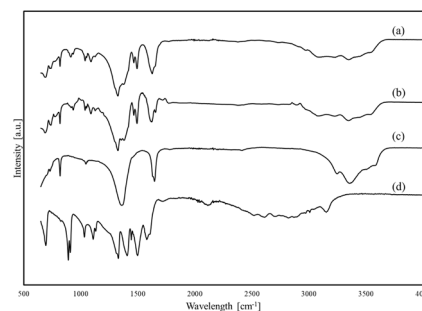


Fig. 3 FTIR of (a) MC formed products, (b) SE formed products, (c) magnesium nitrate hexahydrate, (d) glycine.



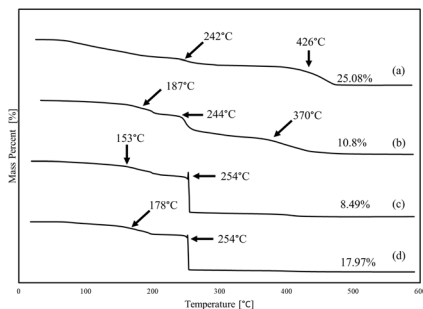


Fig. 4 TGA of (a) physically mixed magnesium nitrate hexahydrate and glycine, (b) 15-minute MC crystals, (c) 30-minute MC crystals, (d) 1-hour MC crystals with each offset by 100%.

synthesis of the complex. The MC crystals largely resemble the SE crystals, with only slight differences in two regions of the spectra. In the $<1250\text{ cm}^{-1}$ region, the relative intensities between peaks that correspond to the constituents vary between the two materials as expected with variations in bonding resulting from the synthesis method, and in the $3000\text{--}3600\text{ cm}^{-1}$ region corresponding to the number of waters of the hydrate. The close resemblance is again a strong indicator that mechanochemical synthesis results in the desired complex.

Simultaneous DSC–TGA was used to further understand the thermal behavior and composition of the MC crystals as a function of mixing time and how they compare to a physical mixture. The TGA/DSC (Fig. 4 and 5) of the physical mixture has an initial mass loss of $\sim 32\%$ at $240\text{ }^\circ\text{C}$ with no significant thermal event up to that point, which is attributed to the dehydration of magnesium nitrate hexahydrate. The later mass loss at $426\text{ }^\circ\text{C}$ closely aligns with the endothermic decomposition of magnesium nitrate hexahydrate beginning at $420\text{ }^\circ\text{C}$.¹⁶ Using eqn (1) and the mass loss at $240\text{ }^\circ\text{C}$, the amount of water present was determined. For the physical mixture, 5.8 waters leave which is close to the expected 6 waters (absent any reaction). After 15 minutes, there was already a significant difference observed in both the mass loss and thermal behavior. The mass loss changed with only $\sim 27\%$ being lost in the 15-minute material at $240\text{ }^\circ\text{C}$ resulting in a calculated water content of 4.5

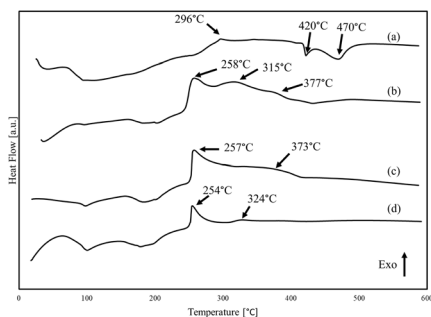


Fig. 5 DSC of (a) physically mixed (1 : 1) magnesium nitrate/glycine, (b) 15-minute MC crystals, (c) 30-minute MC crystals, (d) 1-hour MC crystals. DSCs are normalized and offset to compare when thermal events occur. Full raw data can be found in the SI.

waters which corresponds to a 75% conversion to mgn-gly, significantly lower than the estimation from the Rietveld refinement. The remaining mass loss initiates at $370\text{ }^\circ\text{C}$ closely aligning with a minor exothermic event at $377\text{ }^\circ\text{C}$. The thermal behavior shifted and an exothermic event is observed at $258\text{ }^\circ\text{C}$ corresponding to the decomposition of glycine then two additional events are observed at $315\text{ }^\circ\text{C}$ and $377\text{ }^\circ\text{C}$.¹⁷ The decomposition is exothermic as a result of interactions between the glycine and magnesium nitrate. As milling time increases to 30 minutes the amount of water decreases with $\sim 25\%$ of the mass being lost at $240\text{ }^\circ\text{C}$ representing 4.1 waters corresponding to a 95% conversion to mgn-gly, closely aligning to the Rietveld refinement estimation. The 30-minute MC loses most of its mass at $254\text{ }^\circ\text{C}$ corresponding with an exothermic reaction at $257\text{ }^\circ\text{C}$ once again associated with the decomposition of glycine. The 30-minute sample maintains a secondary exothermic event at $373\text{ }^\circ\text{C}$ but does not correspond to a major mass loss, then a minor mass loss is observed at $418\text{ }^\circ\text{C}$ resulting from the onset of a slight endothermic event at $411\text{ }^\circ\text{C}$, likely the independent decomposition of magnesium nitrate. Finally, the amount of water lost in the 1-hour MC sample was further reduced to $\sim 22\%$ representing 3.5 waters which exceeds the estimated minimum waters of 4. The 1-hour MC sample loses most of its mass at $254\text{ }^\circ\text{C}$ corresponding to the major exothermic event at $254\text{ }^\circ\text{C}$ once again caused by an interaction between the decomposing glycine and the magnesium nitrate. The second exothermic event was minor at $324\text{ }^\circ\text{C}$, significantly less than that of the 30-minute MC. Additionally there is no late endothermic event or further mass loss that would indicate the independent decomposition of magnesium nitrate. As such the synthesis likely reached maximum conversion to the targeted complex after 1 hour of mixing.

$$X = \frac{(1 - W) \cdot \sum Y_i}{MW_{\text{H}_2\text{O}}} \quad (1)$$

Determination of number of water molecules where Y is the stoichiometric value of a molecule times its molecular weight, W is the weight percent lost at $240\text{ }^\circ\text{C}$, $MW_{\text{H}_2\text{O}}$ is the molecular weight of water and X is the number of water molecules.

Simultaneous DSC–TGA was then used to analyze the SE crystal and compare it to the 1-hour MC crystal, the TGA is shown in Fig. 6 and DSC in the supplemental. First, analyzing the water content of the SE crystal using TGA (Fig. 6), a 23% mass loss is observed at $240\text{ }^\circ\text{C}$ representing 3.8 waters, 0.3 more than the 3.5 waters calculated for the 1-hour MC. Though the waters remaining on both materials are less than the minimum of 4, the MC crystal's lower water content suggests a higher conversion to mgn-gly. Additionally, the SE crystal has a late mass loss at $448\text{ }^\circ\text{C}$ corresponding to the independent decomposition of magnesium nitrate.¹⁶ This strongly indicates un-complexed magnesium nitrate decomposing in the SE crystal, which was not observed for the MC crystals.

Finally, the combustion products of both MC and SE crystals were compared. In this work, the specific surface area and the morphology of the combustion products are compared to a solution combustion synthesis route, with the same reaction



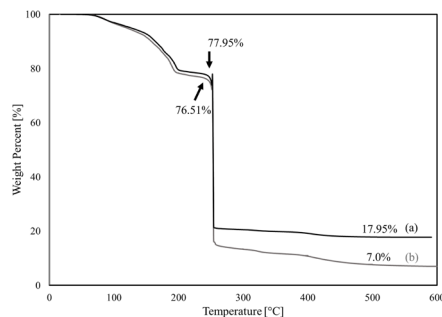


Fig. 6 TGA of (a) MC formed crystal and (b) SE formed crystal.

chemistry. It has been demonstrated that the mgn–gly complex results in enhanced combustion, and as a result, products with surface areas around $20 \text{ m}^2 \text{ g}^{-1}$ were observed.⁴ When the specific surface area of the combustion products is compared (Table 2) a similar surface area was achieved between the MC crystals and the SCS product with the SE crystals achieving a slightly larger specific surface area.

Using mechanochemistry to synthesize energetic complexes can significantly reduce the synthesis time and provide qualitative indicators that a complex has been formed while reducing the screening time for energetic complexes. Additionally, with the metal nitrate shedding its water upon impact with an organic fuel, without the addition of milling media, a simple synthesis method has been demonstrated. The resulting products of the mechanochemical synthesis have less composition variation in the products than the solvent evaporation method making the Lab RAM synthesis a more efficient process from both a time and a product quality perspective. Though this communication focused on a single complex, formed from magnesium nitrate hexahydrate and glycine, this process has worked for many different materials that are capable of producing complexed materials, (hydrated metal nitrates) aluminum nitrate, iron nitrate, nickel nitrate with a variety of organic fuels (hexamine and urea). This process provides an opportunity to produce such materials on a large scale with ease.

The following paragraphs describe the methods used to characterize the synthesized complexes.

Prior to all characterization the crystals were dried at 60° to remove excess moisture associated with the synthesis.

PXRD was conducted on Empyrean Panalytical using a $\text{Co } k\alpha$ radiation source with a tube voltage of 40 kV and tube current of 45 mA. Intensities were taken from 5° to 80° at a scanning rate

of 5° per minute. Data was processed using Jade v 7.0 software, and the resulting diffraction patterns were shifted to a $\text{Cu } k\alpha$ source. PXRD was conducted on the dried synthesized crystals, the dried constituents, and a physical mixture. All materials were ground into a fine powder prior to data analysis.

Fourier transform infrared spectroscopy was conducted with an Agilent Technologies Cary 600 spectrometer with a resolution of 4 cm^{-1} . Resolutions Pro Software generated absorbance intensity at wavelengths from 700 to 4000 cm^{-1} . The resulting data was then plotted in Excel using normalized absorbance intensity *versus* wavelength and offset to compare spectra.

DSC–TGA was conducted on a TA Instruments SDT Q600 to observe the thermal behavior of the materials. This characterization was conducted in open alumina pans with a volume of $90 \mu\text{L}$ with samples between 2 and 2.5 mg. Samples were heated at $20^\circ \text{C min}^{-1}$ with UHP argon flowing at 100 mL min^{-1} from 50 to 600°C . Data analysis was conducted using TA Universal Analysis software.

Moisture analysis was conducted on a Veritas M5-thermo moisture balance. The materials were ground into a powder and examined as received, after being dried at 60°C for three days, and of the final synthesized product. The 1-gram batches of the materials were heated to 100°C and held at that temperature for the maximum runtime of the machine (99 minutes) to ensure time for the materials to undergo a phase change and evaporation of any crystalline water.

The synthesized crystals were ground with a mortar and pestle into a fine powder. The powder was then weighed into half-gram batches and pressed into a half-inch die. The resulting pellet was combusted using a butane torch until the combustion reaction visibly ceased. The products were then collected for further characterization.

BET was conducted upon the combustion products with a Micrometrics Gemini III 2375 Specific Surface Area Analyzer using UHP nitrogen gas and UHP helium gas to measure the free space. Samples were between 0.1 and 0.4 g and were degassed using UHP nitrogen gas at 200°C for 1 hour.

Conflicts of interest

There are no conflicts to declare.

Data availability

The data supporting this article have been included as part of the supplementary information (SI). Supplementary information: moisture content data, additional PXRD and FTIR data, and the Rietveld refinements. See DOI: <https://doi.org/10.1039/d5mr00110b>.

References

- 1 P. Prakash, B. Fall, J. Aguirre, L. A. Sonnenberg, P. Rao Chinnam, S. Chereddy, D. A. Dikin, A. Venkatnathan, S. L. Wunder and a. M. J. Zdilla, *Nat. Mater.*, 2023, **22**, 627–635.

Table 2 The BET-specific surface area of the different heat-treated combustion products from the combustion synthesis of mgn–gly complex

Materials	SSA [$\text{m}^2 \text{ g}^{-1}$]
SE crystals	24 ± 4
MC crystals	21 ± 3
SCS product	21 ± 5



- 2 K. Honer, E. Kalfaoglu, C. Pico, J. McCann and J. Baltrusaitis, *ACS Sustain. Chem. Eng.*, 2017, **5**, 8546–8550.
- 3 V. Nemeč, K. Lisac, N. Bedeković, L. Fotović, V. Stilić and D. Cincić, *CrystEngComm*, 2021, **23**, 3055–3240.
- 4 T. W. Kenny and L. J. Groven, *Mater. Lett.*, 2024, 375.
- 5 E. Irem Senyurt, M. Schoenitz and E. L. Dreizin, *Def. Technol.*, 2021, **17**, 703–714.
- 6 N. Sharma and R. Kakkar, *Adv. Mater. Lett.*, 2013, **4**, 508–521.
- 7 M. Fleck and L. Bohaty, *Acta Crystallogr.*, 2005, **61**, 1887–1889.
- 8 T. Frišćić, *J. Mater. Chem.*, 2010, **20**, 7599–7605.
- 9 A. A. L. Michalchuk, K. S. Hope, S. R. Kennedy, M. V. Blanco, E. V. Boldyreva and C. R. Pulham, *Chem. Commun.*, 2018, **54**, 4033–4036.
- 10 I. Persson, *Pure Appl. Chem.*, 2010, **82**, 1901–1917.
- 11 J. Mahler and I. Persson, *Inorg. Chem.*, 2012, **51**, 425–438.
- 12 I. A. Tumanov, A. A. L. Michalchuk, A. A. Politov, E. V. Boldyreva and V. V. Boldyrev, *CrystEngComm*, 2017, **19**, 2830–2835.
- 13 C. P. Singh, A. Singh, Nibha, C. G. Daniliuc, G. Singh and D. P. Rao, *Biointerface Res. Appl. Chem.*, 2020, **11**, 10895–10905.
- 14 R. L. Mozzi and W. R. Bekebrede, *Acta Crystallogr.*, 1961, **14**, 1296–1297.
- 15 J. Hanawalt, H. Rinn and L. K. Frevel, *Industrial & Chemistry Analytical Edition*, 1938, DOI: [10.1021/AC50125A001](https://doi.org/10.1021/AC50125A001).
- 16 M. R. Reddy, *A Study of the Thermal Decomposition of Some Metal Nitrate Hydrates By Thermal Analysis Techniques*, University of Houston, 1977.
- 17 I. M. Weiss, C. Muth, R. Drumm and H. O. K. Kirchner, *BMC Biophys.*, 2018, **11**, 2.

